Plant Biotechnology 27, 475–480 (2010)

Gene Note

Metal-binding characteristics of the protein which shows the highest histidine content in the *Arabidopsis* genome

Masakazu Hara[1,*], Daiju Kashima[1], Tokumasa Horiike[2], Toru Kuboi[1]

[1] Faculty of Agriculture, Shizuoka University, Shizuoka 422-8529, Japan; [2] Division of Global Research Leaders, Shizuoka University, Shizuoka 422-8529, Japan
* E-mail: masahara@agr.shizuoka.ac.jp Tel & Fax: +81-54-238-5134

Received April 30, 2010; accepted June 18, 2010 (Edited by K. Yazaki)

Abstract It is well documented that metal-binding peptides, such as phytochelatins and metallothioneins, are involved in metal homeostasis and tolerance in plants. These peptides bind metals by means of the thiol groups of cysteine residues. Histidine is also known to be a metal-binding residue. It has been demonstrated that microorganisms and mammals possess histidine-rich metal-binding peptides for the storage and homeostasis of metals. In plants, however, only several examples which describe the characteristics of the histidine-rich metal binding peptides have been reported. We therefore searched for histidine-rich peptides in the *Arabidopsis* database. Here, we describe a candidate gene designated *Arabidopsis thaliana* histidine-rich peptide 1 (AtHIRP1). AtHIRP1, which belongs to a small auxin-up RNA (SAUR) family in *Arabidopsis*, shows the highest histidine content (19.7% of total amino acid residues) in the *Arabidopsis* genome. The recombinant AtHIRP1 apparently bound to Co^{2+}, Ni^{2+}, Cu^{2+}, and Zn^{2+}, but weakly to Cd^{2+}. In the case of the AtHIRP1-Zn^{2+} binding, the dissociation constant was 0.58 μM and the maximum binding capacity was 12 mol Zn^{2+} per 1 mol AtHIRP1. The accumulation of *AtHIRP1* transcripts increased by drought stresses. These results suggest that AtHIRP1 is a metal-binding peptide which may function in plants exposed to abiotic stresses.

Key words: *Arabidopsis thaliana*, histidine, metal-binding, small auxin-up RNA (SAUR).

Many studies have focused on the metal-binding peptides of plants because these peptides are crucial molecules for maintaining metal homeostasis and responding to metal stresses in plants. The metal-binding peptides have also been noted as promising molecules for phytoremediation (Chaney et al. 1997; Pilon-Smits 2005). Phytochelatins and metallothioneins have been well characterized as plant metal-binding peptides (Clemens 2001; Cobbett 2000; Hall 2002; Zenk 1996). Phytochelatins have a general structure (γ-Glu-Cys)$_n$-Gly (n=2–11), and chelate heavy metals, such as Cd and Cu. Metallothioneins are cysteine-rich metal binding peptides which bind to Cu, Zn, and Cd. Both groups of metal binding peptides are believed to be involved in the detoxification of and tolerance to heavy metals, which promote damage in plants when excess doses are supplied (see reviews cited above). A common mechanism of the metal binding by phytochelatins and metallothioneins is that they chelate metals via the thiol groups of cysteine residues.

Microorganisms and mammals, however, have other types of metal-binding peptides to serve various physiological roles. These metal-binding peptides contain little or no cysteine residues, but a high proportion of histidine residues. For example, Hpn, which is a histidine-rich metal-binding peptide in *Helicobacter pylori*, has 28 histidine residues out of 60 amino acids of the total residues (histidine content; 46.7%) (Gilbert et al. 1995). Because Hpn binds Ni^{2+}, Hpn has been proposed to play a role in Ni storage and homeostasis in *H. pylori* to produce Ni-dependent enzymes, such as urease, which is necessary to their gastric infection (Maier et al. 2007; Seshadri et al. 2007). Histatin 5, which is a human salivary metallopeptide showing antimicrobial activity against *Candida albicans*, is 24 amino acids in length and contains 7 histidine residues (histidine content; 29.1%) (Oppenheim et al. 1988). Since histatin 5 can bind Zn^{2+} and Cu^{2+} (Gusman et al. 2001), the peptide has been presumed to contribute to the salivary metal binding capacity. In plants, however, there have only been several reports about histidine-rich metal-binding peptides. AgNt84 is a nodule-specific histidine-rich peptide from the actinorhizal host plant *Alnus glutinosa* (Gupta et al. 2002). AgNt84 has 15 histidine residues out of 99 amino acids in length (histidine content; 15.2%). The AgNt84 bound Co^{2+},

Abbreviations: AtHIRP1, *Arabidopsis thaliana* histidine-rich peptide 1; GFP, green fluorescent protein; IMAC, immobilized metal affinity chromatography; ORF, open reading frame; PCR, polymerase chain reaction; RT-PCR, reverse transcription-polymerase chain reaction; SAUR, small auxin-up RNA; SDS-PAGE, sodium dodecyl sulfate-polyacrylamide gel electrophoresis
This article can be found at http://www.jspcmb.jp/

Ni^{2+}, Cu^{2+}, and Zn^{2+}. *Citrus unshiu* cold-responsive dehydrin, CuCOR15, which shows a rich histidine content (13.9%, 19 histidine residues out of 137 total residues), also bound Co^{2+}, Ni^{2+}, Cu^{2+}, and Zn^{2+} (Hara et al. 2005). Tomato (*Solanum lycopersicum*) abscisic acid stress ripening 1 (ASR1) is a histidine-rich peptide (15.7%, 18 histidine residues out of 115 total residues) which specifically binds to Zn^{2+} (Rom et al. 2006). Both CuCOR15 and ASR1 showed Zn^{2+}-dependent DNA binding (Hara et al. 2009; Kalifa et al. 2004). The metal transporter IRT1 of *Arabidopsis* has the histidine-rich sequence which can bind metal ions (Grossoehme et al. 2006). Although the precise biological functions of the plant histidine-rich metal-binding peptides have not yet been clarified, they may be related to metal homeostasis, metal transport, DNA protection, and regulation of gene expression during nodule development and the stress response.

It is not known whether plants possess histidine-rich metal binding peptides showing higher proportions of histidine residues than AgNt84, CuCOR15, and ASR1. In this paper, we report an *Arabidopsis* gene exhibiting the highest score of the histidine content (19.7%) among the whole open reading frames (ORFs) predicted in the *Arabidopsis* genome. The code of the gene is At5g53590, which belongs to a small auxin-up RNA (SAUR) family. We designated the corresponding ORF *Arabidopsis thaliana* histidine-rich peptide 1 (AtHIRP1). We also show the metal binding characteristics of AtHIRP1.

A recombinant protein which has a His-tag sequence attached to the N-terminus of AtHIRP1 was produced using the pET-30 *Escherichia coli* expression system (Novagen, WI). First, we prepared the *AtHIRP1* cDNA clone by a reverse transcription-polymerase chain reaction (RT-PCR) with the total RNA of *A. thaliana* (L.) Heynh ecotype Columbia (Col-0) by using a Takara RNA PCR kit (Takara, Shiga, Japan). The primer of the RT was an oligo(dT) primer. The primers of the PCR were 5′-ATCTCTAACAACCACCACCG-3′ (a sense primer) and 5′-GATTCTTCCCTTATTCCTCACG-3′ (an antisense primer), which are located in the 5′ and 3′ non-coding regions, respectively. The sequence of the clone was identified as the confirmed sequence of At5g53590 published on The *Arabidopsis* Information Resource site (TAIR; http://www.arabidopsis.org/). The ORF of *AtHIRP1* obtained by a PCR from the cDNA clone was inserted into the ligation-independent cloning (LIC) site. The LIC which is a cloning system without ligation was performed in accordance with the manufacturer's instructions (Novagen). The first methionine of *AtHIRP1* starts directly after the tag in the frame, and the translation stops by using the stop codon of *AtHIRP1*. *E. coli* strain BL21 containing the expression construct was precultured at 37°C. After adding 1 mM isopropyl β-D-thiogalactopyranoside to the culture, the incubation proceeded for an additional 3 h at 28°C. Bacterial cells were lysed by treating with BugBuster reagent (Novagen). Because the tagged recombinant protein was insoluble, the supernatant was discarded and the pellet was then washed three times with BugBuster reagent. The washed pellet was solubilized with 6 M guanidine hydrochloride. The sample was loaded onto a 1-ml HiTrap Chelating HP (GE Healthcare Biosciences, Tokyo, Japan) column charged with Ni^{2+}. After washing the column with 5 ml of a washing buffer (25 mM Tris-HCl pH 8.0 containing 500 mM NaCl, 20 mM imidazole, 1 mM 2-mercaptoethanol, and 6% 6 M urea), the retained protein was refolded by reducing the urea concentration of the washing buffer. The program of the stepwise gradient of the urea was as follows, 5, 4, 3, 2, and 1 M urea-containing buffers (3 ml each) in order, and then 6 ml of the washing buffer without urea. Finally, the soluble, tagged recombinant protein was obtained by adding an elution buffer (3 ml, 25 mM Tris-HCl pH 8.0 containing 500 mM NaCl, 500 mM imidazole, and 1 mM 2-mercaptoethanol) to the column. A solution of the protein sample was changed to a storage buffer (1/2EQ buffer) consisting of 25 mM Tris-HCl and 500 mM NaCl (pH 7.5) using a NAP-25 column (GE Healthcare Biosciences). The tag attached to AtHIRP1 was removed using a Factor Xa Kit (Novagen) in accordance with the manufacturer's instructions. The tag-less AtHIRP1 was purified using the 1-ml HiTrap Chelating HP column charged with Ni^{2+}. The tag-less AtHIRP1 fraction was subjected to the NAP-25 column equilibrated with 1/2EQ buffer. The tag-less AtHIRP1 protein was identified by a nano-liquid chromatography–mass spectrometry system composed of QSTAR XL (Applied Biosystems, Tokyo, Japan) and Bio NanoLC (KYA Technologies, Tokyo, Japan). The sequences of fragments were matched to the corresponding partial sequences of AtHIRP1 by considering their molecular weights.

The bindings of AtHIRP1 to divalent cations were analyzed by immobilized metal affinity chromatography (IMAC). The HiTrap Chelating HP column was used with a stepwise gradient of imidazole (1 ml of 150 mM, 1 ml of 200 mM, 1 ml of 250 mM, 1 ml of 300 mM, 1 ml of 350 mM, 1 ml of 400 mM, 1 ml of 450 mM, and 2 ml of 500 mM). Fractions (0.5 ml each) were analyzed using sodium dodecyl sulfate-polyacrylamide gel electrophoresis (SDS-PAGE). The gel was stained with Coomassie Brilliant Blue. The band intensities of AtHIRP1 in the SDS-PAGE gels were calculated using NIH-image software (National Institutes of Health, MD) to produce the graphs. The binding between AtHIRP1 and Zn^{2+} was analyzed using an ultrafiltration method described by Hara et al. (2005). The filtration device was Ultrafree-MC (5000 NMWL, Millipore, MA). The Zn^{2+}

```
AtHIRP1     1:MGFEENQKQSPKQSPNHIKHMVFKFHFHVPH-LHILPHHHHHHHHDVPKGCVAIMVGHEDDEEGLHRFVVPLVFLSHPLFLDLLKEAEKE 89
AAM1        1:MGTGE------K---T-LKS----FQLHRKQSVKVK---------DVPKGCLAIKVGSQGEEQQ--RFIVPVLYFNHPLFMQLLKEAEDE 65
SAUR-AC1    1:MA---------------------F----LRS--FLGAKQIIRRESSSTPRGFMAVYVGENDQKKK--RYVVPVSYLNQPLFQQLLSKSEEE 62
S44175      1:MG---------------------FRLPGIRKASFSAN-QASSKAVDVEKGYLAVYVGEKMR-----RFVIPVSYLNKPSFQDLLSQAEEE 63
                *                                          *  *  **        *   *       * *  **   * *

AtHIRP1    90:YGFKHD-GPITIPCGVDEFKHVQEVIDEETHRRHSHGGHGHNN-HNHHNN--HLR-CF--                              142
AAM1       66:YGFDQK-GTITIPCHVEEFRYVQALIDGERSVY--NGN-NHHHRHGGRDQYHHLVGCFRA                              121
SAUR-AC1   63:FGYDHPMGGLTIPCHESLFFTVTSQIQ-------------------------------                              89
S44175     64:FGYHHPNGGLTIPCSEDVFQHITSFLN-------------------------------                              90
              *     *  ****     *
```

Figure 1. Alignment of amino acid sequences between AtHIRP1 and related small auxin-up RNA (SAUR) proteins. Proteins are *Arabidopsis* AtHIRP1 (AtSAUR30, At5g53590, in this study), *Arabidopsis* AAM1 (AtSAUR32, At2g46690), *Arabidopsis* SAUR-AC1 (AtSAUR15, At4g38850), and soybean S44175. A grey background represents a conserved domain among SAUR proteins. Two histidine-rich domains in AtHIRP1 were enclosed by open squares. An underline shows a histidine-rich domain in AAM1. Asterisks represent amino acid identity between the four sequences.

concentration was determined using a 2-(5-Bromo-2-pyridylazo)-5-(*N*-propyl-*N*-sulfopropylamino)phenol (5-Br-PAPS) (Dojindo Chemical, Tokyo, Japan) assay (Makino et al. 1982). The free Zn^{2+} concentration (F) was used to calculate the bound Zn^{2+} concentration (B). Next, the B/F value and how many Zn^{2+} atoms AtHIRP1 were bound in each sample were determined. Finally, the Scatchard plots, i.e., the number of Zn^{2+} atoms (*x*-axis) versus the B/F value (*y*-axis), were drawn to obtain the values of K_d and B_{max}.

First, we searched for an open reading frame (ORF) which shows the highest histidine content from the *Arabidopsis* genome. We downloaded the *Arabidopsis* ORF data (33,200 ORFs) from the National Center for Biotechnology Information (NCBI) site to search for histidine-rich peptides. After the histidine contents of the whole ORFs were calculated, the top 10 candidates were listed (Supplemental data 1). The ORF with the highest histidine content was *At5g53590* (accession; NP_200171). The *At5g53590* encoded 142 amino acids containing 28 histidine residues (histidine content: 19.7%). The deduced molecular weight was 16678. Because of the high histidine content, we designated the gene *A. thaliana histidine-rich peptide 1* (*AtHIRP1*). Information from the TAIR indicated that *AtHIRP1*, i.e. *At5g53590*, belongs to a small auxin-up RNA (SAUR) gene family. Hagen and Guilfoyle (2002) applied AtSAUR numbers to categorize the *Arabidopsis* SAUR genes. The AtSAUR number of AtHIRP1 is AtSAUR30.

Figure 1 shows the alignment between AtHIRP1 and the related SAURs at the amino acid level. Although AtHIRP1 possesses a central sequence which is conserved in SAURs (Figure 1, grey background), the peptide has extensive sequences to the N- and C-terminus which are varied among the different SAURs. The N- and C-terminus extensive sequences of AtHIRP1 contain histidine-rich domains (enclosed by open squares). *Arabidopsis abolished apical hook maintenance 1* (*AAM1*), which is related to the apical hook development (Park et al. 2007), also has a similar histidine-rich domain at the C-terminus (underline). To

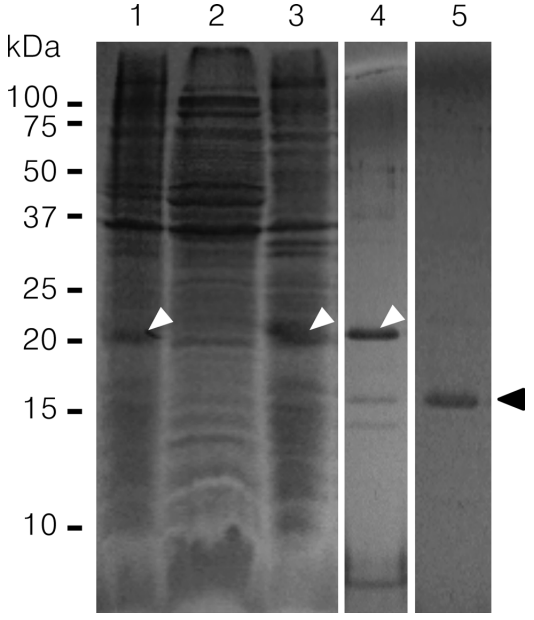

Figure 2. Production of a recombinant AtHIRP1 protein using the *Escherichia coli* expression system. Proteins at the different production steps were analyzed by SDS-PAGE. Lane 1; crude extract of bacterial cells (100 ng), lane 2; soluble fraction of bacterial lysis (100 ng), lane 3; insoluble fraction of bacterial lysis (100 ng), lane 4; recombinant tagged AtHIRP1 protein (5 ng), and lane 5; recombinant tag-less AtHIRP1 protein (5 ng). The tagged (open arrowheads) and the tag-less (a closed arrowhead) AtHIRP1 proteins are shown.

investigate the metal-binding properties of AtHIRP1, we produced the recombinant protein by means of the *E. coli* system (Figure 2). The ORF of AtHIRP1 was inserted into the pET-30 vector plasmid directly after the tag sequence in the frame. The calculated molecular weights of the His-tagged protein and the tag-less protein were 21632 and 16678, respectively. A protein of approximately 21 kDa, which was likely to be the tagged protein, was produced in the bacterial cells that had the pET-30 plasmid containing the AtHIRP1 ORF (Figure 2, lane 1, open arrowhead). Since the tagged protein was considered to exist as an inclusion body in the insoluble fraction (Figure 2, lane 3, open arrowhead), we solubilized the insoluble protein by the refolding process

(Figure 2, lane 4, open arrowhead). After the tag was removed by the Factor Xa digestion, an approximately 16 kDa protein was obtained (Figure 2, lane 5, closed arrowhead). The nanoLC-MS/MS analysis of the protein band indicated that the AtHIRP1-related sequences, such as M(1)GFEENQKQSPK(12), G(49)CVAIMVGHEDDEEGLHRFVVPLVFLSHPLFLDLLK(84), and H(94)DGPITIPCGVDEFKHVQEVIDEETHRR(121) were identified (53% coverage). This demonstrates that the band is the recombinant AtHIRP1 protein.

The IMAC was performed to investigate whether AtHIRP1 can bind metals. When AtHIRP1was applied to the column chelating Mg^{2+}, Ca^{2+}, Mn^{2+}, Co^{2+}, Ni^{2+}, Cu^{2+}, Zn^{2+}, or Cd^{2+}, AtHIRP1 was shown to be retained in the column immobilizing Co^{2+}, Ni^{2+}, Cu^{2+}, Zn^{2+}, or Cd^{2+} (data not shown). However, AtHIRP1 passed through the columns immobilizing Mg^{2+}, Ca^{2+}, and Mn^{2+}. In order to find out the difference of the binding strengths between AtHIRP1 and the five metals, i.e., Co^{2+}, Ni^{2+}, Cu^{2+}, Zn^{2+}, and Cd^{2+}, elution with a stepwise gradient of the imidazole concentration was performed in the IMAC (Figure 3A). Such IMAC assays have been used to evaluate the strength of the metal-binding of proteins via the histidine residues, because the separation of proteins is mainly based on forces acting between their amino acid residues and the metal ions (Ueda et al. 2003). The elution of AtHIRP1 from the Zn^{2+} column continued even when the imidazole concentration reached 450–500 mM. The amount of AtHIRP1 which was eluted from the Zn^{2+} column by the imidazole concentration (450–500 mM) was approximately 18% of the total amount of AtHIRP1 applied to the column. However, the AtHIRP1 elution from the Co^{2+}, Ni^{2+}, and Cu^{2+} columns was completed until 400 mM imidazole. A lower concentration of imidazole (62.5 mM) was sufficient to elute AtHIRP1 from the Cd^{2+} column (data not shown). These results suggest that AtHIRP1 may prefer Zn^{2+} most among the five metals tested. In plants, Zn content (approximately 20 mg kg^{-1} dry weight) is known to be much higher than the contents of Co (approximately 1 mg kg^{-1} dry weight), Ni (approximately 0.1 mg kg^{-1} dry weight), and Cu (approximately 6 mg kg^{-1} dry weight), whereas the contents can vary widely depending on plant species and environmental conditions (Palit et al. 1994; Palmer and Guerinot 2009). Taken together, we decided to perform following tests with Zn^{2+}. The Scatchard plots analysis of the binding between AtHIRP1 and Zn^{2+} indicated that the binding proceeded with the two binding modes (Figure 3B). The dissociation constants of a higher affinity binding and a lower one were 0.58 μM and 380 μM, respectively. The maximum binding was approximately 12 mol Zn^{2+} mol^{-1} AtHIRP1.

In this study, we found that an ORF showing the

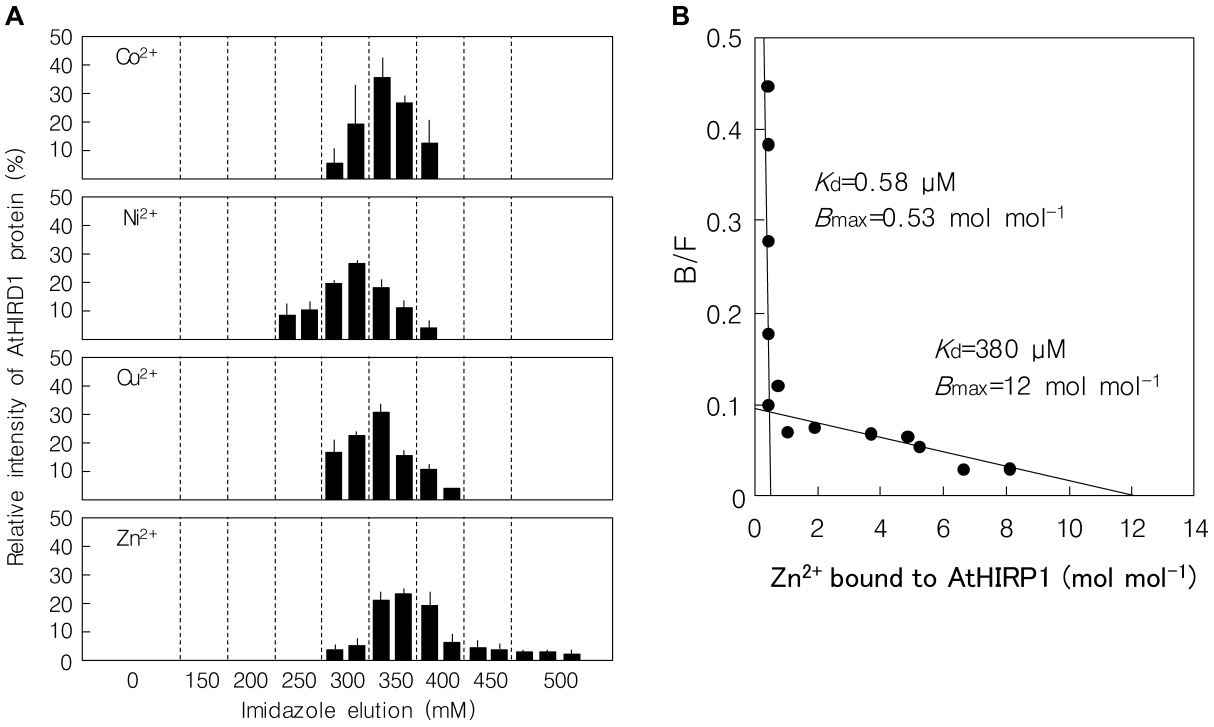

Figure 3. Binding of AtHIRP1 to metal ions. (A) Immobilized metal affinity chromatography (IMAC) analyses were performed to test binding between AtHIRP1 and Co^{2+}, Ni^{2+}, Cu^{2+}, and Zn^{2+}. A tag-less AtHIRP1 protein retained in each metal column was eluted by a stepwise gradient of imidazole, and then fractions were analyzed using SDS-PAGE. The gel was stained with Coomassie Brilliant Blue. Band intensities of AtHIRP1 in the SDS-PAGE gel were shown as relative intensities of AtHIRP1 (total intensity; 100%). Values and bars represent means and SD of three independent experiments, respectively. (B) Scatchard plots in the binding between AtHIRP1 and Zn^{2+} are shown.

highest proportion of histidine content in *Arabidopsis* is *AtHIRP1* (*At5g53590*) by *in silico* screening of the *Arabidopsis* genome database. The content of histidine residues in AtHIRP1 was 19.7%. Since the occurrence of histidine residues in general proteins is approximately 2% (Ueda et al. 2003), it was noted that AtHIRP1 is a remarkably histidine-rich peptide. AtHIRP1 bound to Zn^{2+} as well as AgNt84, CuCOR15, and ASR1. Information about the Zn^{2+}-binding characteristics and histidine contents in plant histidine-rich metal-binding peptides is summarized (Table 1). At present, it can be noted that AtHIRP1 shows the highest histidine content, the highest B_{max}, and the lowest K_d among the plant histidine-rich peptides investigated.

AtHIRP1 belongs to the SAUR family, which was primarily found as auxin-responsive genes expressed at the elongation zone of soybean hypocotyls treated with auxin (McClure et al. 1989). The function of SAUR has been unknown, but recent studies have shown insights into the putative functions. Analyses of transgenic rice overexpressing the *SAUR39* gene suggest that SAUR39 acts as a negative regulator for auxin synthesis and transport (Kant et al. 2009). The *Arabidopsis SAUR32* gene, which is a synonym of *AAM1*, is related to the apical hook development. The transgenic *Arabidopsis* overexpressing *AAM1* showed a hookless phenotype which was completely rescued by exogenous auxin (Park et al. 2007). These results suggest that *SAUR* genes may contribute to the growth and development of plants by influencing the synthesis and transport of auxin. Other than those results, the characteristics of SAUR proteins have not been documented except for studies showing that maize and *Arabidopsis* SAUR proteins bind to calmodulin (Reddy et al. 2002; Yang and Poovaiah 2000). In the present study, it was demonstrated that AtHIRP1 is a metal-binding protein. Since the metal binding was canceled by imidazole, two histidine-rich domains (Figure 1, enclosed by open squares) in the N- and C-terminuses may be related to the binding.

Table 1. Zinc ion binding constants and histidine contents of histidine-rich metal binding peptides in plants.

	AtHIRP1	AgNt84-6	CuCOR15	ASR1
Zinc ion binding				
B_{max} (mol mol^{-1})	12	4	12	2
K_d (μM)	0.6	1.7	5.1	n.d.
Histidine contents				
Total amino acids	142	99	137	115
Histidine numbers	28	15	19	18
Histidine contents (%)	20	15	14	16

The peptides are *Arabidopsis thaliana* AtHIRP1 (this study), *Alnus glutinosa* AgNt84-6 (Gupta et al. 2002), *Citrus unshiu* CuCOR15 (Hara et al. 2005), and *Solanum lycopersicum* ASR1 (Rom et al. 2006). B_{max} and K_d values of AtHIRP1, AgNt84-6, and CuCOR15 were determined by equilibrium methods. B_{max} value of ASR1 was obtained by matrix-assisted laser desorption/ionization mass spectrometry. n.d.; not determined.

Although *Arabidopsis* possesses over 70 SAUR genes, it is not known how many genes are expressed and auxin-inducible (Hagen and Guilfoyle 2002). Because the transcripts accumulation of *AtHIRP1* was not affected by indole-3-acetic acid (Supplemental data 2), *AtHIRP1* seems to be an auxin-insensitive *SAUR*. This does not contradict the data that there is no typical auxin-responsive element in at least the 1000 bp upstream region of the *AtHIRP1* gene when the region was investigated at the PLACE website (http://www.dna.affrc.go.jp/PLACE/signalscan.html) (data not shown). On the one hand, the gene expression of *AtHIRP1* was enhanced by drought, abscisic acid, and mannitol (Supplemental data 2). The enhancing effects of cold and mannitol on the *AtHIRP1* expression were exhibited in the eFP *Arabidopsis* browser (http://bbc.botany.utoronto.ca) (Winter et al. 2007). This shows that the *AtHIRP1* expression may be controlled by signals related to water stresses. In fact, there are various *cis* elements related to drought, abscisic acid, and cold (data not shown). We investigated which kinds of genes are coexpressed with *AtHIRP1* by searching the ATTED-II website (http://www.atted.bio.titech.ac.jp) (Obayashi et al. 2007). Interestingly, the scheme of the 'coexpressed gene network' in the website represented that three histidine-rich peptide genes, *At5g17650* (histidine content; 18.5%), *At4g19200* (histidine content; 12.9%), and *At5g45350* (histidine content; 10.7%), are closely linked to the *AtHIRP1* gene. This means that one set of histidine-rich peptide genes including *AtHIRP1* may be coexpressed by the same stimuli in *Arabidopsis*. The SOSUI (http://bp.nuap.nagoya-u.ac.jp/sosui/) membrane prediction system suggested that AtHIRP1 is a soluble protein. AtHIRP1 was predicted to be localized to cytoplasm, plasma membrane, endoplasmic reticulum, and chloroplast by the PSORT system (http://www.psort.org/). Subcellular localization analyses using transient expression of green fluorescent protein (GFP)-related constructs, such as, the *AtHIRP1-GFP* expression construct, the *GFP* expression construct (Chiu et al. 1996; Niwa 2003), the plastid-targeting *GFP* expression construct (Engprasert et al. 2004), and the mitochondria-targeting *GFP* expression construct (Chang et al. 1999) in onion (*Allium cepa*) epidermal cells suggest that AtHIRP1 is likely distributed in the plastids (Supplemental data 3).

Above we described the biochemical and physiological characteristics of AtHIRP1, such as the binding to metals and the gene expression enhanced by the dehydration-related stimuli. Further studies are needed to elucidate the biological roles of AtHIRP1.

Acknowledgements

We would like to thank Dr. Y. Niwa (Shizuoka Prefectural

University) for providing *35S-Ω-sGFP*, *35S-Ω-pt-sGFP*, and *35S-Ω-pre-sGFP*. We would also like to thank Dr. H. Dohra (Shizuoka University) for helpful suggestions on the use of confocal laser-scanning microscopy. This work was supported by a Grant-in-Aid for Scientific Research from the Ministry of Education, Science and Culture of Japan (19380182).

References

Chaney RL, Malik M, Li YM, Brown SL, Brewer EP, Angle JS, Baker AJ (1997) Phytoremediation of soil metals. *Curr Opin Biotechnol* 8: 279–284

Chang CC, Sheen J, Bligny M, Niwa Y, Lerbs-Mache S, Stern DB (1999) Functional analysis of two maize cDNAs encoding T7-like RNA polymerases. *Plant Cell* 11: 911–926

Chiu W, Niwa Y, Zeng W, Hirano T, Kobayashi H, Sheen J (1996) Engineered GFP as a vital reporter in plants. *Curr Biol* 6: 325–330

Clemens S (2001) Molecular mechanisms of plant metal tolerance and homeostasis. *Planta* 212: 475–486

Cobbett CS (2000) Phytochelatins and their roles in heavy metal detoxification. *Plant Physiol* 123: 825–832

Engprasert S, Taura F, Kawamukai M, Shoyama Y (2004) Molecular cloning and functional expression of geranylgeranyl pyrophosphate synthase from *Coleus forskohlii* Briq. *BMC Plant Biol* 4: 18

Gilbert JV, Ramakrishna J, Sunderman FW Jr, Wright A, Plaut AG (1995) Protein Hpn: cloning and characterization of a histidine-rich metal-binding polypeptide in *Helicobacter pylori* and *Helicobacter mustelae*. *Infect Immun* 63: 2682–2688

Grossoehme NE, Akilesh S, Guerinot ML, Wilcox DE (2006) Metal-binding thermodynamics of the histidine-rich sequence from the metal-transport protein IRT1 of *Arabidopsis thaliana*. *Inorg Chem* 45: 8500–8508

Gupta RK, Dobritsa SV, Stiles CA, Essington ME, Liu Z, Chen CH, Serpersu EH, Mullin BC (2002) Metallohistins: a new class of plant metal-binding proteins. *J Protein Chem* 21: 529–536

Gusman H, Lendenmann U, Grogan J, Troxler RF, Oppenheim FG (2001) Is salivary histatin 5 a metallopeptide? *Biochim Biophys Acta* 1545: 86–95

Hagen G, Guilfoyle T (2002) Auxin-responsive gene expression: genes, promoters and regulatory factors. *Plant Mol Biol* 49: 373–385

Hall JL (2002) Cellular mechanisms for heavy metal detoxification and tolerance. *J Exp Bot* 53: 1–11

Hara M, Fujinaga M, Kuboi T (2005) Metal binding by citrus dehydrin with histidine-rich domains. *J Exp Bot* 56: 2695–2703

Hara M, Shinoda Y, Tanaka Y, Kuboi T (2009) DNA binding of citrus dehydrin promoted by zinc ion. *Plant Cell Environ* 32: 532–541

Kalifa Y, Gilad A, Konrad Z, Zaccai M, Scolnik PA, Bar-Zvi D (2004) The water- and salt-stress-regulated Asr1 (abscisic acid stress ripening) gene encodes a zinc-dependent DNA-binding protein. *Biochem J* 381: 373–378

Kant S, Bi YM, Zhu T, Rothstein SJ (2009) SAUR39, a small auxin-up RNA gene, acts as a negative regulator of auxin synthesis and transport in rice. *Plant Physiol* 151: 691–701

Maier RJ, Benoit SL, Seshadri S (2007) Nickel-binding and accessory proteins facilitating Ni-enzyme maturation in *Helicobacter pylori*. *Biometals* 20: 655–664

Makino T, Saito M, Horiguchi D, Kina K (1982) A highly sensitive colorimetric determination of serum zinc using water-soluble pyridylazo dye. *Clin Chim Acta* 120: 127–135

McClure BA, Hagen G, Brown CS, Gee MA, Guilfoyle TJ (1989) Transcription, organization, and sequence of an auxin-regulated gene cluster in soybean. *Plant Cell* 1: 229–239

Niwa, Y (2003) A synthetic green fluorescent protein gene for plant biotechnology. *Plant Biotechnol* 20: 1–11

Obayashi T, Kinoshita K, Nakai K, Shibaoka M, Hayashi S, Saeki M, Shibata D, Saito K, Ohta H (2007) ATTED-II: a database of co-expressed genes and *cis* elements for identifying co-regulated gene groups in *Arabidopsis*. *Nucleic Acids Res* 35 (Database issue): D863–869

Oppenheim FG, Xu T, McMillian FM, Levitz SM, Diamond RD, Offner GD, Troxler RF (1988) Histatins, a novel family of histidine-rich proteins in human parotid secretion. Isolation, characterization, primary structure, and fungistatic effects on *Candida albicans*. *J Biol Chem* 263: 7472–7477

Palit S, Sharma A, Talukder G (1994) Effects of Cobalt on Plants. *Bot Rev* 60: 149–181

Palmer CM, Guerinot ML (2009) Facing the challenges of Cu, Fe and Zn homeostasis in plants. *Nat Chem Biol* 5: 333–340

Park JE, Kim YS, Yoon HK, Park CM (2007) Functional characterization of a *small auxin-up RNA* gene in apical hook development in *Arabidopsis*. *Plant Sci* 172: 150–157

Pilon-Smits E (2005) Phytoremediation. *Annu Rev Plant Biol* 56: 15–39

Reddy VS, Ali GS, Reddy AS (2002) Genes encoding calmodulin-binding proteins in the *Arabidopsis* genome. *J Biol Chem* 277: 9840–9852

Rom S, Gilad A, Kalifa Y, Konrad Z, Karpasas MM, Goldgur Y, Bar-Zvi D (2006) Mapping the DNA- and zinc-binding domains of ASR1 (abscisic acid stress ripening), an abiotic-stress regulated plant specific protein. *Biochimie* 88: 621–628

Seshadri S, Benoit SL, Maier RJ (2007) Roles of His-rich hpn and hpn-like proteins in *Helicobacter pylori* nickel physiology. *J Bacteriol* 189: 4120–4126

Ueda EK, Gout PW, Morganti L (2003) Current and prospective applications of metal ion-protein binding. *J Chromatogr A* 988: 1–23

Winter D, Vinegar B, Nahal H, Ammar R, Wilson GV, Provart NJ (2007) An "Electronic Fluorescent Pictograph" browser for exploring and analyzing large-scale biological data sets. *PLoS One* 2: e718

Yang T, Poovaiah BW (2000) Molecular and biochemical evidence for the involvement of calcium/calmodulin in auxin action. *J Biol Chem* 275: 3137–3143

Zenk MH (1996) Heavy metal detoxification in higher plants-a review. *Gene* 179: 21–30